Physics of Atomic Nuclei, Vol. 66, No. 8, 2003, pp. 1586–1589. From Yadernaya Fizika, Vol. 66, No. 8, 2003, pp. 1629–1632.

Multidimensional Langevin Approach to Description of Near-Barrier Heavy-Ion Fusion and Deep-Inelastic Collisions*

M. A. Naumenko**, **A. S. Denikin, and V. I. Zagrebaev**

Joint Institute for Nuclear Research, Dubna, Moscow oblast, 141980 Russia

Received August 28, 2002

Abstract—A six-dimensional Langevin approach is developed for the analysis of near-barrier heavy-ion fusion and deep-inelastic collisions. In its framework, vibrational and rotational degrees of freedom of both nuclei are taken into account explicitly. Calculated fusion cross sections, compound nuclei spin distributions, and angular and energy distributions of deep-inelastic products show satisfactory agreement with experimental data. © *2003 MAIK "Nauka/Interperiodica".*

1. INTRODUCTION

Fokker–Planck and Langevin equations may be successfully applied for the description of low-energy fusion and deep-inelastic collisions. These equations are based on the concepts of nuclear friction and stochastic behavior of the system with many degrees of freedom. The solution of the Langevin equations is less difficult compared to the Fokker–Planck equation and does not require additional simplifying assumptions. It is well known that the deformations of nuclear surfaces and the rotation of deformed nuclei seriously affect the dynamics of nuclear interaction. Therefore, taking them into account is important for the description of low-energy nucleus–nucleus collisions. But this dramatically increases the calculation time and difficulty, which is the main reason why up to now only two- or four-dimensional calculations have been performed [1]. In the present work, vibrational and rotational degrees of freedom of both nuclei are taken into account explicitly in the framework of the six-dimensional Langevin approach. Fusion cross sections, compound nuclei spin distributions, and angular and energy distributions of deep-inelastic products are calculated and compared with experimental data.

2. THEORETICAL MODEL

Collective degrees of freedom play a significant role in low-energy ($\leq$10 MeV/nucleon) fusion and deep-inelastic collisions. For the description of these processes, a six-dimensional Langevin model may be applied. The geometry of collision is shown schematically in Fig. 1. Let us assume for simplicity that the symmetry axes of nuclei belong to the plane of reaction. We shall use the following notation: r is the distance between centers of mass of nuclei, θ is the polar angle, φ_i are the angles between the symmetry axes of the nuclei and the beam direction, β_i are the dynamic quadrupole deformations, β_{i0} are the static quadrupole deformations of the ground states, $q = \{r, \theta, \varphi_i, \beta_i\}$ is the complete set of six variables, and $p_r, p_\theta, p_{\varphi_i}$, and p_{β_i} are the conjugated momenta. We suppose that the index $i = 1$ corresponds to the projectile, and $i = 2$ to the target. Let us also introduce angles $\alpha_1 = \varphi_1 + \theta$ and $\alpha_2 = \varphi_2 - \theta$.

The surface of the deformed axially symmetric nucleus taking into account volume conservation may be described by the formula

$$R_i(\alpha_i, \beta_i) = \frac{R_{i0}(1 + \beta_i Y_{20}(\alpha_i))}{\sqrt[3]{1 + \frac{3}{5}\delta_i^2 + \frac{2}{35}\delta_i^3}}, \qquad (1)$$

where $R_{i0} = r_{i0}A_i^{1/3}$, $\delta_i = \sqrt{5/(4\pi)}\beta_i$, and $Y_{20}(\alpha_i)$ is a spherical harmonic of the second order. In our calculations, we chose the parameter $r_0 = 1.2$ fm for both nuclei.

To describe surface vibrations of nuclei we will use the harmonic oscillator model. The corresponding Lagrangians may be written in the form

$$L_i^{\text{vib}} = \frac{p_{\beta_i}^2}{2B_i} - C_i\frac{(\beta_i - \beta_{i0})^2}{2}, \qquad (2)$$

where C_i are the rigidity parameters and B_i are the mass parameters; they may be calculated in the framework of the liquid drop model or from experimental data about vibrational states of nuclei.

*This article was submitted by the authors in English.

**e-mail: naumenko@lnr.jinr.ru

1063-7788/03/6608-1586$24.00

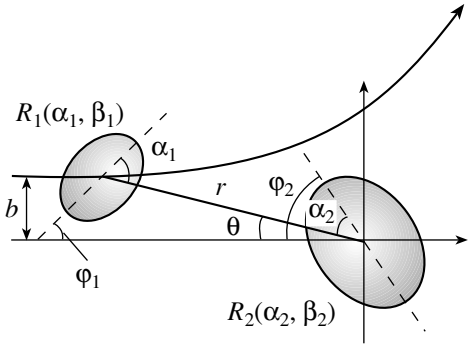

Fig. 1. The geometry of the collision process.

The full Lagrangian is then

$$L = \frac{p_r^2}{2\mu} + \frac{p_\theta^2}{2\mu r^2} + \sum_i \frac{p_{\varphi_i}^2}{2J_i} + \sum_i \left(\frac{p_{\beta_i}^2}{2B_i} - C_i \frac{(\beta_i - \beta_{i0})^2}{2} \right) - V(q), \tag{3}$$

where μ is the reduced mass of the system; J_i are the inertia momenta of nuclei; and V is the interaction potential, which consists of Coulomb and nuclear parts.

The Coulomb interaction is a sum of monopole–monopole and monopole–quadrupole interactions, $V_C = V_C^{(mm)} + V_C^{(mq)}$. The monopole–monopole one was chosen in the form

$$V_C^{(mm)} = Z_1 Z_2 e^2 \begin{cases} 1/r, & r > R_C, \\ (3 - r^2/R_C^2)/(2R_C), & r < R_C, \end{cases} \tag{4}$$

where $R_C = R_{01} + R_{02}$. We shall denote the quadrupole momenta of nuclei by Q_i; then,

$$V_C^{(mq)} = \frac{Z_1 Q_2 e^2}{2R^2} P_2(\cos\alpha_2) f(q) + \frac{Z_2 Q_1 e^2}{2R^2} P_2(\cos\alpha_1) f(q), \tag{5}$$

where

$$Q_i \approx \frac{3}{\sqrt{5\pi}} Z_i \widetilde{R}_i^2 \beta_i, \quad R = \widetilde{R_1} + \widetilde{R_2},$$

$$\widetilde{R_i} = R_{0i} \Big/ \sqrt[3]{1 + \frac{3}{5}\delta_i^2 + \frac{2}{35}\delta_i^3},$$

$$f(q) = \begin{cases} R^2/r^3, \ r > \widetilde{R_1}(1+\delta_1) + \widetilde{R_2}(1+\delta_2), \\ r^2/R^3, \ r < \widetilde{R_1}(1-\delta_1/2) + \widetilde{R_2}(1-\delta_2/2), \\ s^2(q)R^2/r^3 + c^2(q)r^2/R^3, \ \text{in other cases.} \end{cases}$$

Here, $s^2(q) + c^2(q) = 1$, and functions $s(q)$ and $c(q)$ are chosen so that $f(q)$ is continuous together with its first derivative.

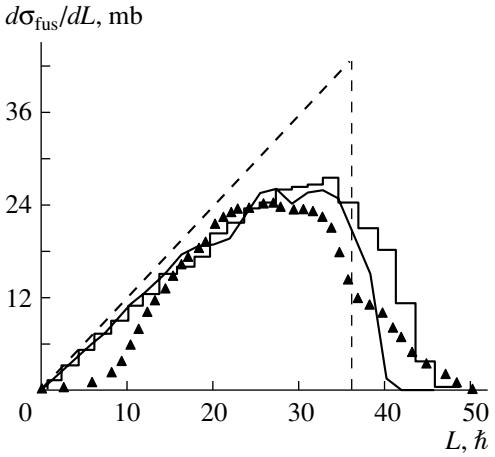

Fig. 2. The compound nuclei spin distribution for the reaction $^{16}O(E_{c.m.} = 80.4$ MeV$) + {}^{144}Nd \to {}^{160}Er^*$. The experimental data (triangles) are compared with theoretical calculations by Fröbrich [5] (histogram) and our results obtained with and without fluctuations (solid and dashed lines, respectively).

Woods–Saxon potentials with volume or surface form factors or a "proximity" potential [2] may be chosen as the nuclear part of the interaction. We must note that all potentials will give almost the same fusion cross sections, compound nuclei spin distributions, and angular and energy distributions of deep-inelastic products if positions and heights of their barriers are the same. In our calculations, the Woods–Saxon volume potential

$$V_N(q) = V_0 \frac{1}{1 + \exp[(r - R_V)/a]} \tag{6}$$

is used, where $R_V = R_1(\alpha_1, \beta_1) + R_2(\alpha_2, \beta_2)$ and the diffuseness parameter $a = 0.5$ fm.

Phenomenological nuclear friction is introduced to describe the dissipation of kinetic energy into degrees of freedom that are not taken into account explicitly within this model (mostly single-particle ones). The Rayleigh function is written in the standard form

$$D = \frac{1}{2} \sum_{k,n=1}^{6} \gamma_{kn}(q) \dot{q}_k \dot{q}_n, \tag{7}$$

where $\gamma_{kn}(q)$ is the friction tensor calculated within the surface friction model [3].

Friction leads to the heating of nuclei and appearance of stochastic forces $F_k(t) = \sqrt{\gamma_{kk} T}\Gamma(t)$, where $\Gamma(t)$ is a Gaussian-distributed random value with the following properties: $\langle \Gamma(t) \rangle = 0$ and $\langle \Gamma(t)\Gamma(t') \rangle = 2\delta_\varepsilon(t - t')$ (see, for example, [1]); the temperature of the nuclei $T = \sqrt{E^*/d}$ is determined by the excitation energy E^* and the level density parameter $d = (A_1 + A_2)/8$ MeV^{-1} [4].

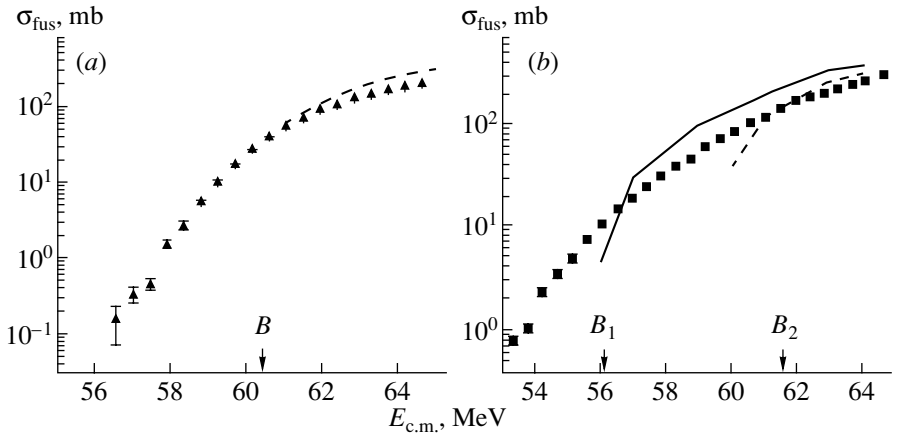

Fig. 3. (*a*) The excitation function for the reaction $^{16}O + {}^{144}Sm$. Triangles represent experimental data [6], and the dashed line is our calculation for spherical nuclei. (*b*) The excitation function for the reaction $^{16}O + {}^{154}Sm$. Squares represent experimental data [6]; the dashed line is our calculation for spherical nuclei; the solid line is our calculation taking into account static deformation of ^{154}Sm with averaging over initial orientations.

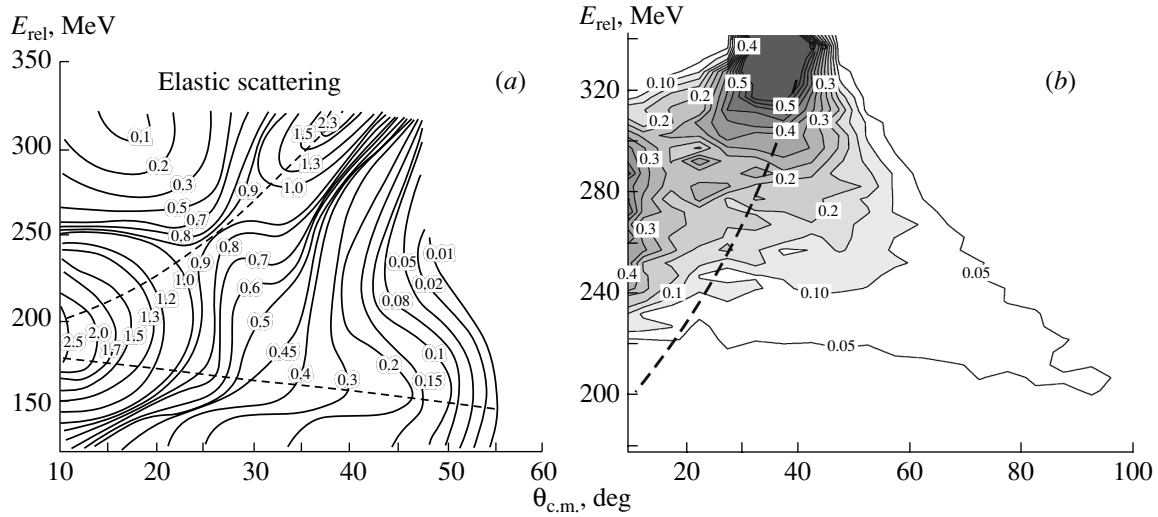

Fig. 4. Double differential cross section (in mb/(sr MeV)) for the reaction $^{56}Fe(E_{c.m.} = 345\ MeV) + {}^{165}Ho$. (*a*) Experiment [7]; projectile-like fragments with $12 \leq Z \leq 35$ were detected. (*b*) Calculation; stochastic forces were taken into account.

The set of Langevin equations

$$\frac{d}{dt}\left(\frac{\partial L}{\partial \dot{q}_k}\right) - \frac{\partial L}{\partial q_k} = -\frac{\partial D}{\partial \dot{q}_k} + \sqrt{\gamma_{kk}(q)\,T(E^*)}\,\Gamma(t),\ k = \overline{1,6}, \tag{8}$$

is solved numerically. The incident energy, impact parameter, deformations, and orientations of the nuclei are the initial conditions that we need for its solution. In case of stochastic forces, for each impact parameter, a number of trajectories are calculated. Those of them that go far enough behind the potential barrier cannot go outside and contribute to the fusion cross section. Others go outside or even may be reflected from the barrier without overcoming it, which leads the system to deep-inelastic, quasi-elastic, or elastic channels. In the case of deformed ground states, averaging over randomly chosen initial orientations is performed.

3. RESULTS OF OUR CALCULATIONS

The feature mentioned above results in smearing-out of calculated compound nuclei spin distributions, which allows us to reproduce the corresponding experimental data successfully. The compound nuclei spin distribution for the reaction $^{16}O(E_{c.m.} = 80.4\ MeV) + {}^{144}Nd \rightarrow {}^{160}Er^*$ is given in Fig. 2. The experimental data (triangles) are compared with theoretical calculations by Fröbrich [5] (histogram)

and with our results obtained with and without fluctuations (solid and dashed lines, respectively). In spite of the fact that only relative motion degrees of freedom were included in our calculations, the results show good agreement with experiment and Fröbrich's calculations performed taking into account dynamic deformations and using "nose-to-nose" geometry.

Rotational degrees of freedom are very important in the case of highly deformed nuclei collisions. A good example of this fact is a significant difference in the fusion cross sections of ^{16}O with two isotopes ^{144}Sm and ^{154}Sm. The ground state of ^{144}Sm is spherically symmetric, but ^{154}Sm is highly deformed with quadrupole deformation $\beta_{20} = 0.27$. In the latter case, instead of one Coulomb barrier, we obtain a multidimensional potential surface strongly depending on the orientation of the colliding nuclei. The excitation functions for the fusion reactions $^{16}\mathrm{O} + {}^{144}\mathrm{Sm}$ and $^{16}\mathrm{O} + {}^{154}\mathrm{Sm}$ are given in Fig. 3. Triangles and squares represent experimental data [6], dashed lines are calculations for spherical nuclei, and the solid line in Fig. 3*b* is a calculation taking into account the static deformation of ^{154}Sm with averaging over initial orientations. In Fig. 3*a*, the Coulomb barrier for spherical nuclei is marked with an arrow, and in Fig. 3*b*, the barriers B_1 and B_2 correspond to the different orientations of the target $\alpha_2 = 0°$ and 90°, respectively. The role of rotation and dynamic deformation is much less in this case; including them hardly changes the results. We can see that static deformation of ^{154}Sm plus averaging over initial orientations allows one to obtain fusion events at subbarrier energies, which leads to better agreement with experimental data. The Langevin forces do not significantly influence the fusion cross section in this case because of the low excitation energy, i.e., low temperature of the touching nuclei.

In calculation of deep-inelastic processes with energies about 10 MeV/nucleon, stochastic forces play a much more noticeable role and taking them into account is necessary for a realistic description of energy and angular distributions of fragments. The experimental double differential cross section (Wylczynski plot) for the reaction $^{56}\mathrm{Fe}(E_{\mathrm{cm}} = 345\ \mathrm{MeV}) + {}^{165}\mathrm{Ho}$ is given in Fig. 4*a*. In the experiment projectile-like fragments with $12 \leq Z \leq 35$ were detected. The results of our calculation are shown in Fig. 4*b*. Here, stochastic forces were taken into account without dynamic rotations and deformations. A pronounced ridge is observed in the experimental data. It is shown as a dashed line in both figures. We see that the model properly reproduces the position of the maximum in the double differential cross section corresponding to so-called grazing collisions. The main reason for the discrepancy between theoretical calculations and experiment for large energy losses is the nucleon exchange in the collision process, which we did not take into account. This will be our immediate task for the future.

4. CONCLUSION

A six-dimensional Langevin approach is proposed for description of near-barrier fusion and deep-inelastic collisions. The role of vibrational and rotational degrees of freedom in the dynamics of nucleus–nucleus collisions was investigated. It was shown that taking them into account is important for reproducing the experimental data because the interaction potential strongly depends on these degrees of freedom. Taking into account fluctuations allows one to reproduce compound nuclei spin distributions without influencing much the value of the fusion cross section. Stochastic forces also play an important role in forming angular and energy distributions of the fragments formed in deep-inelastic processes.

The solution of the Langevin equations gives us important information about the dissipated energy, dynamic deformations, and orientations of nuclei at the moment of their contact, which is important for the analysis of the system's further evolution into channels of complete fusion and deep-inelastic scattering.

Nucleon exchange plays an important role in the dynamics of heavy-ion collision. Taking into account additional degrees of freedom describing nucleon exchange is our immediate task for the future.

REFERENCES

1. P. Fröbrich and I. I. Gontchar, Phys. Rep. **292**, 131 (1998).
2. J. Blocki, J. Randrup, W. J. Swiatecki, and C. F. Tsang, Ann. Phys. (N.Y.) **105**, 427 (1977).
3. D. H. E. Gross and H. Kalinowski, Phys. Rep. C **45**, 175 (1978).
4. A. V. Ignatyuk, *Statistical Properties of Excited Atomic Nuclei* (Énergoizdat, Moscow, 1983).
5. P. Fröbrich, Springer Proc. Phys. **58**, 93 (1991).
6. J. R. Leigh *et al.*, Phys. Rev. C **52**, 3151 (1995).
7. A. D. Hoover *et al.*, Phys. Rev. C **25**, 256 (1982).